SCAR-AWARE LATE MECHANICAL ACTIVATION DETECTION NETWORK FOR OPTIMAL CARDIAC RESYNCHRONIZATION THERAPY PLANNING

Jiarui Xing[a] *Shuo Wang*[d] *Amit R. Petal*[d]
Kenneth C. Bilchick[d] *Frederick H. Epstein*[c] *Miaomiao Zhang*[a,b]

[a] Department of Electrical and Computer Engineering, University of Virginia, USA
[b] Department of Computer Science, University of Virginia, USA
[c] Department of Biomedical Engineering, University of Virginia Health System, USA
[d] School of Medicine, University of Virginia Health System, USA

2025 IEEE 22nd International Symposium on Biomedical Imaging (ISBI) | 979-8-3315-2052-6/25/$31.00 ©2025 IEEE | DOI: 10.1109/ISBI60581.2025.10980862

ABSTRACT

Accurate identification of late mechanical activation (LMA) regions is crucial for optimal cardiac resynchronization therapy (CRT) lead implantation. However, existing approaches using cardiac magnetic resonance (CMR) imaging often overlook myocardial scar information, which may be mistakenly identified as delayed activation regions. To address this issue, we propose a scar-aware LMA detection network that simultaneously detects myocardial scar and prevents LMA localization in these scarred regions. More specifically, our model integrates a pre-trained scar segmentation network using late gadolinium enhancement (LGE) CMRs into a LMA detection network based on highly accurate strain derived from displacement encoding with stimulated echoes (DENSE) CMRs. We introduce a novel scar-aware loss function that utilizes the segmented scar information to discourage false-positive detections of late activated areas. Our model can be trained with or without paired LGE data. During inference, our model does not require the input of LGE images, leveraging learned patterns from strain data alone to mitigate false-positive LMA detection in potential scar regions. We evaluate our model on subjects with and without myocardial scar, demonstrating significantly improved LMA detection accuracy in both scenarios. Our work paves the way for improved CRT planning, potentially leading to better patient outcomes.

1. INTRODUCTION

The accurate detection of LMA regions in the heart is crucial for optimizing CRT in patients with heart failure [1, 2, 3]. LMA detection directly impacts treatment outcomes by guiding the optimal placement of CRT lead [4, 5]. Precise identification of these regions is essential for improving cardiac function and patient quality of life. An Initial effort proposed a semi-automatic approach based on active contour [5], the widespread use of which is limited by its requirement of intense data-specific parameter tuning and its limited accuracy. A breakthrough is made with the introduction of deep learning methods that enabled fully automatic LMA detection [6]. Building on this foundation, researchers have continued to refine these techniques, incorporating multitask learning strategies [7] to leverage related cardiac analysis tasks, and developing multimodal approaches that combine strain prediction with LMA detection [8], resulting in significant accuracy improvements. Despite these advances, the accuracy of current methods remains limited due to the lack of consideration for myocardial scar tissue, which regions can produce strain patterns similar to those of LMA, potentially misleading detection algorithms.

To address these challenges, we propose a novel scar-aware LMA detection network that effectively integrates myocardial scar information predicted from pre-trained segmentation networks. Our framework includes two key components: (i) a scar segmentation network using paired LGE CMRs, and (ii) an LMA detection network utilizing strain data derived from DENSE CMRs. We introduce a novel loss function, which effectively suppresses false-positive LMA detection in areas identified as scar regions. The segmented scar maps are well utilized to guide the LMA detection network to focus more accurately on delayed activated scar-free regions, minimizing the influence of scar-induced motion abnormalities. Our model is designed to be flexible, allowing training with data that may or may not include corresponding LGE images. This enables the use of a larger and more diverse training dataset. In the inference stage, LGE images are not required, making the model more practical for widespread clinical application. We tested our approach on real cardiac MR images and compared it with the state-of-the-art deep learning LMA detection method [7]. Experimental results show that our proposed method achieves improved LMA detection accuracy, especially when myocardial scar presents.

2. BACKGROUND

Building strain matrix. Instead of directly using strain video, we first build strain matrices, which represent my-

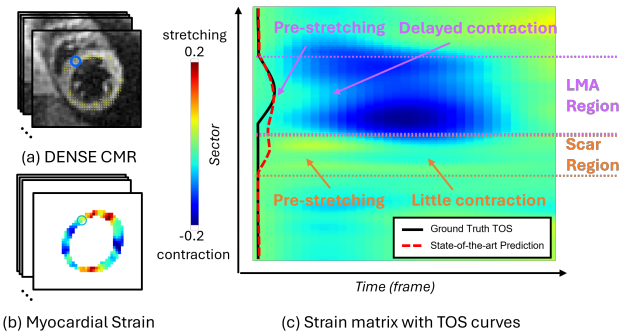

Fig. 1. An example of (a) DENSE CMR data (b) corresponding myocardial strain (c) corresponding strain matrix with TOS curves from manually labeling and current start-of-the-art model, where the later incorrectly treat scar region as LMA region.

ocardial contraction in a relatively low-dimensional space, reducing the cost of network training and risk of overfitting. From DENSE image sequences of T_s frames (Fig. 1(a)), we first compute circumferential strain along the myocardium (Fig. 1(b)). We then evenly divide the myocardium region into N_s sectors, which forms a strain vector of corresponding frame. The sectors are indexed counter-clockwise, starting from the middle of the intersection points between the left and right ventricles (marked with blue circles in Fig. 1(a) and (b)). We then construct a $N_s \times T_s$ strain matrix by concatenating all strain vectors across time.

Quantify LMA with TOS. The time to the onset of circumferential shortening (TOS) of each sector is used to quantify the activation time, as TOS has been shown to have a close linear relationship with electrical activation time [9]. Higher TOS values indicate more severe delayed activation (Fig. 1(c)) [9, 1]. LMA regions typically exhibit a distinct pattern of pre-stretching (yellow) followed by late activation (blue), as shown in Fig. 1(c).

Challenges from myocardial scarring. Scarred regions can cause early stretching patterns similar to LMA, potentially misleading detection algorithms. Although these regions also show a distinct pattern of little to no contraction in later frames, current methods often fail to differentiate this from true LMA. Fig. 1(c) demonstrates how existing algorithms can be misled by the early stretching in scar regions.

3. METHODOLOGY

Our proposed scar-aware LMA detection network contains two key components: a scar segmentation network and an LMA prediction network with a novel scar-aware loss function. This integrated approach enhances LMA detection accuracy by accounting for the presence of myocardial scar tissue. An overview of our proposed scar-aware LMA detection framework is shown in Fig. 2.

Scar segmentation network. We build on recent work in myocardial scar segmentation [10], which performs joint segmentation of the myocardium and scar tissue. This approach improves scar segmentation accuracy by masking out background regions, leading to more precise identification of scar areas. The network predicts myocardium segmentation $\hat{M}_M$ from a given LGE CMR image I, then uses $\hat{M}_M$ to weight I before generating scar segmentation $\hat{M}_S$. The loss function combines myocardium segmentation loss L_M and scar segmentation loss L_S:

$$L_{\text{seg}} = \sum_{i=1}^{N_{\text{seg}}} \lambda_M L_M \left(M_{Mi}, \hat{M}_{Mi}; I_i\right) + \lambda_S L_S \left(M_{Si}, \hat{M}_{Si}; \hat{M}_{Mi} \odot I_i\right), \quad (1)$$

where $\odot$ represents element-wise prediction. L_M and L_S are defined as a weighted sum of cross-entropy and Dice loss, respectively. The training site size is denoted by N_{seg} and i represents the data index.

Scar-aware LMA prediction network. The LMA prediction network takes the highly accurate strain matrices derived from DENSE CMR images as input, and predicts corresponding TOS curves, which representing the activation time along the myocardium. The key of our approach is the scar-aware TOS prediction loss function, which is designed to suppress false-positive LMA predictions in scarred regions. To compute the loss, we first convert the predicted scar segmentations into scar vectors $\hat{S} \in [0, 1]$ representing scarring ratios within each myocardial sector (e.g., the ratio of scarred pixels to total myocardium pixels in each sector), and they serve as weighting parameters in the LMA detection network. Let T and $\hat{T}$ represent the ground-truth and predicted TOS curves, respectively. Noting $\emptyset_s$ as the scarring sectors and $\emptyset_{sf}$ as the scar-free sectors, we formulate the scar-aware loss function as follows:

$$L = \sum_{i=1}^{N} \left[\|T_{i,j\in\emptyset_{sf}} - \hat{T}_{i,j\in\emptyset_{sf}}\|_2^2 + \lambda(1 + \hat{S}_{i,j\in\emptyset_s}) \|\hat{T}_{i,j\in\emptyset_s}\|_2^2 \right], \quad (2)$$

where N denotes the number of training data samples, i is the data index and j is the myocardial sector index. $\hat{S}_{i,j\in\emptyset_s}$ represents the non-zero scarring ratios, and λ is a weighting parameter. This loss function encourages accurate TOS prediction in scar-free regions while penalizing non-zero predictions in scarred areas, effectively minimizing the influence of scar-induced motion abnormalities on LMA detection.

Our model is flexible in requiring LGE CMRs. In scenarios where LGE CMR images are unavailable or unnecessary, the model defaults to standard LMA detection [6]. This allows the network to be trained on a mixture of data with and without LGE images. Moreover, once trained, the network can operate without additional LGE images during inference.

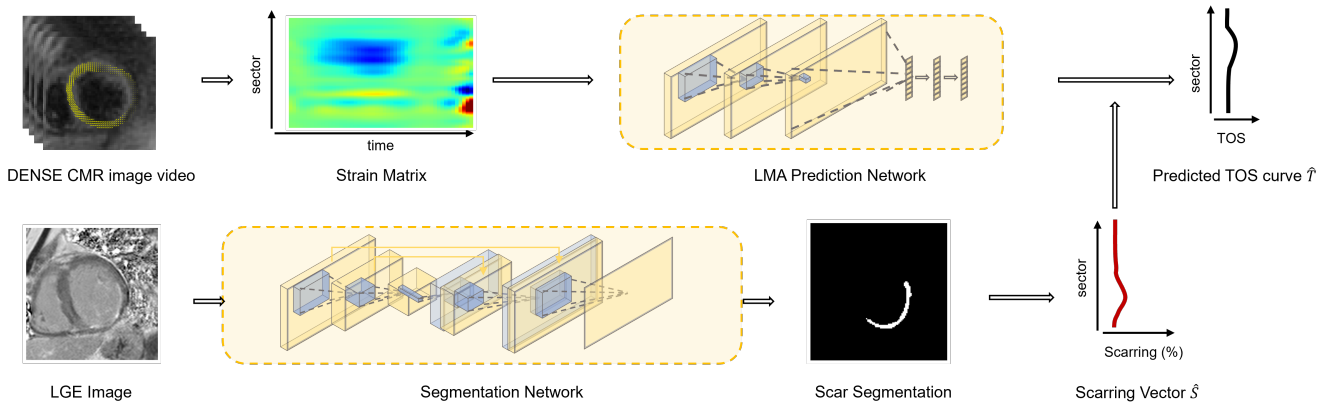

Fig. 2. An overview of our proposed scar-aware LMA detection framework.

This adaptable design ensures that our scar-aware LMA detection network can be applied across various clinical scenarios, maintaining high detection accuracy while adapting to the available imaging data. As a result, it serves as a versatile tool for improving cardiac resynchronization therapy planning.

4. EXPERIMENT

We validate our method on DENSE strain data paired with LGE images. We compare out model with the state-of-the-art LMA detection approach [7].

Data acquisition. The LGE CMRs were acquired with pixel size of 1.5 mm^2 and slice thickness=8mm. All LGE images have corresponding manually labeled scar segmentation from experts. The myocardial strain is computed from the displacement field collected from cine DENSE scans. The DENSE data was performed in 4 short-axis planes at basal, two mid-ventricular, and apical levels (with temporal resolution of 17 ms, pixel size of 2.65^2 mm^2, and slice thickness=8mm). Other parameters included displacement encoding frequency $k_e = 0.1$ cycles/mm, flip angle $15°$, and echo time $= 1.08$ ms. All the strain matrices are aligned to 40 temporal frames with zero padding or clipping. All of the ground-truth TOS curves are manually labeled by experts.

Experimental settings. In our experiment, we first pre-trained the scar segmentation model with 510 LGE images from 140 subjects. We then train the LMA detection network on short-axis DENSE slices, using predicted scar maps from the pre-trained segmentation model. 342 DENSE slices from 71 subjects were used, which are divided into 216 slices for training, 54 for validation, and 72 for testing from different subsets of subjects. Among these, 33 slices with myocardial scarring (with over 50% transmurality) have corresponding LGE images, 13 of which are used for testing. Note that when testing, LGE images are not provided to the models as input. Instead they are used only to identify the scar regions and evaluate how much the models are misled by scars.

We first quantitatively compare the accuracy our scar-aware model with the baseline algorithm, using TOS ($N = 128$) mean absolute error as the evaluation metric. The TOS values are shifted so that TOS=0ms if no LMA exists. We then visually compare the 3D activation maps reconstructed from the TOS prediction. We also built 3D scarring maps from the scar segmentation, which show the scarring regions on the 3D myocardial surface and can be used to identify whether the model successfully avoid making false-positive LMA prediction at scarring region.

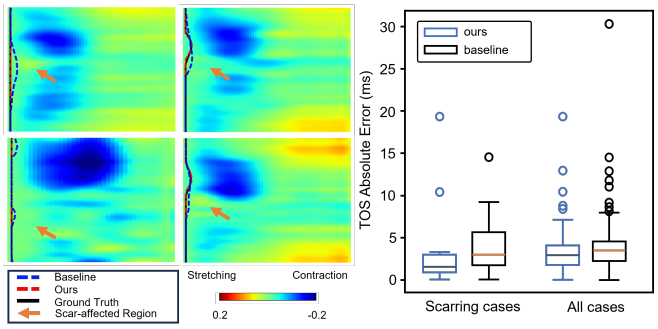

Fig. 3. Left: Visualization of four examples comparing the predicted and ground-truth TOS. Right : A boxplot comparison TOS error.

Experimental results. The left panel of Fig. 3 shows examples of TOS prediction from the compared methods as well as the ground truth, where the scar-affected region are marked with the arrows. It shows that our scar-aware network managed to tell the scarring region from LMA region, and avoid making false-positive predictions, while the baseline method was mislead by the scar pre-stretch pattern. The right panel of Fig. 3 displays quantitative results of TOS error, demonstrating that our model outperforms the baseline in predicting TOS in both scarred (2.36 (0.98, 3.18)ms vs. 4.60 (3.49, 8.07)ms) cases and overall cases (2.87 (1.72, 4.08)ms vs. 3.46 (2.27, 4.57)ms).

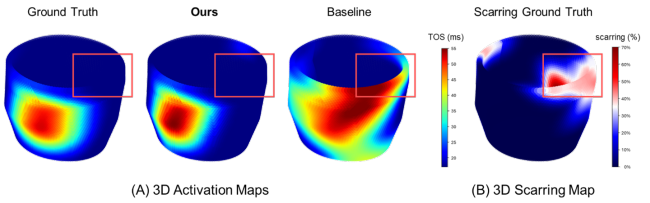

Fig. 4. (A) 3D visualization of activation maps generated from ground truth and predicted TOS. (B) 3D scarring map of the same subject. A notable scar is marked with red bounding box, which our model identifies from LMA region, while the baseline misidentifies it as an LMA region.

Fig. 4 visualizes 3D LMA maps using predicted TOS from our model and the baseline, compared to manually labeled ground-truth TOS. Regions with TOS large values (marked with red rectangles) indicate severe late activation. The 3D scarring map built from the ground-truth scar segmentation of the same subject is also provided. It shows that the baseline method is mislead by the scarring region in the basal inferolateral (marked with a red rectangle) while our method made much more accurate prediction.

5. CONCLUSION

In this paper, we present a novel scar-aware LMA detection network that addresses a key limitation of current methods by incorporating myocardial scar information. Our approach well utilizes scar segmentations from LGE data to benefit the LMA detection based on DENSE-derived strain data, resulting in substantially improved LMA detection accuracy, especially in cases involving myocardial scarring. Our model's capability to distinguish LMA regions from scar-induced motion abnormalities, along with its flexibility to operate with or without LGE data, enhances its clinical utility. This advancement in LMA detection accuracy holds promise for optimizing CRT lead implantation planning, supporting more informed decision-making, and potentially improving outcomes for heart failure patients receiving CRT.

Compliance with ethical standards. This work was supported by NIH 1R21EB032597. All studies involving human subjects and waiver of consent were approved by our institutional review board.

6. REFERENCES

[1] K. C. Bilchick, D. A. Auger, M. Abdishektaei, R. Mathew, M.-W. Sohn, X. Cai, C. Sun, A. Narayan, R. Malhotra, A. Darby, et al., "Cmr dense and the seattle heart failure model inform survival and arrhythmia risk after crt," *Cardiovascular Imaging*, vol. 13, no. 4, pp. 924–936, 2020.

[2] L. P. Budge, A. S. Helms, M. Salerno, C. M. Kramer, F. H. Epstein, and K. C. Bilchick, "Mr cine dense dyssynchrony parameters for the evaluation of heart failure: comparison with myocardial tissue tagging," *JACC: Cardiovascular Imaging*, vol. 5, no. 8, pp. 789–797, 2012.

[3] R. Borgquist, W. R. Barrington, Z. Bakos, A. Werther-Evaldsson, and S. Saba, "Targeting the latest site of left ventricular mechanical activation is associated with improved long-term outcomes for recipients of cardiac resynchronization therapy," *Heart Rhythm O2*, vol. 3, no. 4, pp. 377–384, 2022.

[4] K. C. Bilchick, S. Kuruvilla, Y. S. Hamirani, R. Ramachandran, S. A. Clarke, K. M. Parker, G. J. Stukenborg, P. Mason, J. D. Ferguson, J. R. Moorman, et al., "Impact of mechanical activation, scar, and electrical timing on cardiac resynchronization therapy response and clinical outcomes," *Journal of the American College of Cardiology*, vol. 63, no. 16, pp. 1657–1666, 2014.

[5] R. Ramachandran, X. Chen, C. M. Kramer, F. H. Epstein, and K. C. Bilchick, "Singular value decomposition applied to cardiac strain from mr imaging for selection of optimal cardiac resynchronization therapy candidates," *Radiology*, vol. 275, no. 2, pp. 413–420, 2015.

[6] J. Xing, S. Ghadimi, M. Abdi, K. C. Bilchick, F. H. Epstein, and M. Zhang, "Deep networks to automatically detect late-activating regions of the heart," in *2021 IEEE 18th International Symposium on Biomedical Imaging (ISBI)*. IEEE, 2021, pp. 1902–1906.

[7] J. Xing, S. Wang, K. C. Bilchick, F. H. Epstein, A. R. Patel, and M. Zhang, "Multitask learning for improved late mechanical activation detection of heart from cine dense mri," in *2023 IEEE 20th International Symposium on Biomedical Imaging (ISBI)*. IEEE, 2023, pp. 1–5.

[8] J. Xing, N. Wu, K. C. Bilchick, F. H. Epstein, and M. Zhang, "Multimodal learning to improve cardiac late mechanical activation detection from cine mr images," in *2024 IEEE International Symposium on Biomedical Imaging (ISBI)*. IEEE, 2024, pp. 1–4.

[9] B. T. Wyman, W. C. Hunter, F. W. Prinzen, and E. R. McVeigh, "Mapping propagation of mechanical activation in the paced heart with mri tagging," *American Journal of Physiology-Heart and Circulatory Physiology*, vol. 276, no. 3, pp. H881–H891, 1999.

[10] J. Xing, S. Wang, K. C. Bilchick, A. R. Patel, and M. Zhang, "Joint deep learning for improved myocardial scar detection from cardiac mri," in *2023 IEEE 20th International Symposium on Biomedical Imaging (ISBI)*. IEEE, 2023, pp. 1–5.